High-Frequency Behavior and Damping of Fe–Co–N-Based High-Saturation Soft Magnetic Films

N. X. Sun, S. X. Wang, T. J. Silva, *Member, IEEE*, and A. B. Kos

***Abstract*—Magnetization dynamics measurements at subnanosecond time scale have been performed on Fe–Co–N high-saturation soft magnetic films with Permalloy nanolayer seeds and having a saturation magnetization of 1.9 MA/m (1900 emu/cm^3). The damping parameter α varies from 0.011 to 0.018, depending on applied bias field. The peak frequencies of the imaginary permeability spectra and the zero-crossing frequencies of the real permeability spectra cannot be fitted with a fixed value of anisotropy field, indicating that the Kittel equation is only qualitatively valid for these films. A phenomenological damping criterion is established based on a small-signal solution of the Landau–Lifshitz–Gilbert equation: critical damping occurs in a soft magnetic film when the damping parameter is $\alpha = 2/\sqrt{\chi_0}$, where χ_0 is the initial permeability. The experimentally observed damping parameters are smaller than the critical value for the range of bias fields employed. The Fe–Co–N-based films have a ferromagnetic resonance frequency of 2 GHz at zero-bias field, showing great promise for applications in write heads and integrated inductors in a frequency range >1 GHz.**

***Index Terms*—damping parameter, Fe-Co-N film, ferromagnetic resonance, Landau–Lifshitz–Gilbert equation, magnetic thin film.**

I. Introduction

SOFT magnetic films with low coercivity and high permeability are critical building blocks in numerous electromagnetic devices such as magnetic recording heads, integrated inductors, and micromachined motors. However, a lack of soft magnetic materials with a high saturation magnetization (>1.6 MA/m) and a large permeability rolloff frequency (>1 GHz) often becomes the bottleneck in these applications. In particular, we are approaching the perceived superparamagnetic limit of magnetic recording. Many high anisotropy magnetic media are capable of accommodating areal densities of >15.5 Gb/cm^2 (100 Gb/in^2), but they are not practical because magnetic write heads cannot produce sufficiently large and sharp fields to record useful data on them.

We have developed Fe–Co–N based materials with Permalloy nanolayer seeds that are very promising for applications as write head pole materials. Their properties are summarized in Table I, where B_s is the saturation flux density, H_c the hard axis coercivity, H_k the in-plane anisotropy field, ρ the resistivity, χ_0 the initial susceptibility along the hard axis, and $f_{3\,\mathrm{dB}}$ the 3 dB rolloff frequency of the real part of the hard axis susceptibility. The details regarding the fabrication and soft magnetism of these materials have been published elsewhere [1], [2].

TABLE I
PROPERTIES OF Fe–Co–N FILMS WITH PERMALLOY NANOLAYER SEEDS

B_s (T)	H_c (A/m)	H_k (kA/m)	χ_0	ρ ($\mu\Omega$·cm)	$f_{3\mathrm{dB}}$ (GHz)
2.4	< 80	1.6	1200	50	1.5

With the continued advance of data rate in magnetic disk drives, the high-frequency performance of soft magnetic thin films becomes increasingly important [3]–[5]. Improved understanding of the high-frequency behavior for soft films will facilitate high data-rate magnetic recording (and integrated inductors) at frequencies in excess of 1 GHz. Therefore, we investigated the high frequency behavior and damping of the Fe–Co–N-based films by performing magnetization dynamics measurements at a subnanosecond time scale.

II. Experiment

The magnetization dynamics of Fe–Co–N films were studied with a pulsed inductive microwave magnetometer (PIMM) [4]. The apparatus is composed of a pulse generator and an oscilloscope connected by a waveguide, on which a magnetic film is placed. The whole system has an effective bandwidth of 6 GHz. Two sets of biasing Helmholtz coils provide the DC fields parallel and perpendicular to the waveguide direction. The electrical pulse produces an excitation field perpendicular to the waveguide according to Ampere's law. The magnetic film on the waveguide responds to the excitation, and the inductive voltage generated by the time-varying magnetization along the excitation direction is recorded by the oscilloscope in the time domain. The inductive time-domain data were analyzed to obtain the Landau–Lifshitz damping parameter α. Frequency domain analysis was used to obtain the permeability spectrum. (Relative permeability and susceptibility differ by unity, but they are indistinguishable for unsaturated soft ferromagnetic materials.) Both the *zero-crossing frequency* of the real permeability spectrum ω_0 and the *peak frequency* of the imaginary permeability spectrum ω_p were determined. They are a good measure of the ferromagnetic resonance frequency of the films. In this work, the amplitude of the *step magnetic field* is chosen to be about 200 A/m (2.5 Oe), which is much smaller than the anisotropy

Manuscript received July 3, 2001. The work at Stanford was supported in part by the National Science Foundation under Grant no. ECS-0096704.

N. X. Sun and S. X. Wang are with the Center for Research on Information Storage Materials (CRISM), Stanford University, Stanford, CA 94305-4045 USA (e-mail: nxsun@stanford.edu; sxwang@ee.stanford.edu).

T. J. Silva and A. B. Kos are with the National Institute of Standards and Technology (NIST), Boulder, CO 80305 USA.

Publisher Item Identifier S 0018-9464(02)02184-2.

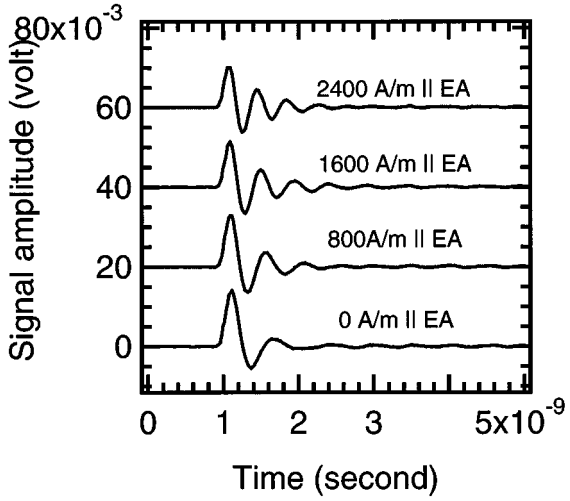

Fig. 1. Time domain signals for the Fe–Co–N film on Permalloy underlayer at different longitudinal bias fields: 0, 800, 1600, and 2400 A/m (0, 10, 20, and 30 Oe), all showing underdamped behavior. Note that signal amplitudes have been shifted upwards with respect to the 0 A/m bias field curve for better illustration. EA is easy-axis.

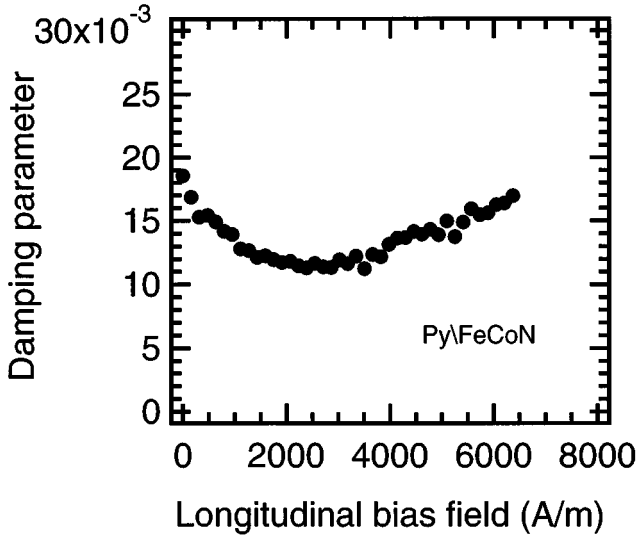

Fig. 2. Damping parameter as a function of the longitudinal bias field for the Fe–Co–N thin films on Permalloy underlayer.

field of 1600 A/m (20 Oe). The magnetization oscillates with an angular amplitude of less than 130 mrad under such an excitation field, satisfying the *small-signal* condition. The samples analyzed here are made of a 100-nm-thick Fe–Co–N film on a 2 nm Permalloy underlayer (referred to as Py/FeCoN). The Permalloy nanolayer helps to achieve a low dispersion angle and a low hard-axis coercivity in the Fe–Co–N layer [1], [2].

Typical time domain signals with different longitudinal bias fields are shown in Fig. 1. As expected, the signal oscillates faster as the longitudinal bias field is increased, indicating that the precessional frequency (or the ferromagnetic resonance frequency) of these films increases. This trend is similar to the results on Permalloy films [4]. All signals show a sinusoidal oscillation with an exponentially decreasing envelope, indicative of *underdamped* behavior. This will be discussed further in Section III.

The damping parameters are obtained by fitting the time-domain data with an exponentially decaying sinusoidal curve [4]. As shown in Fig. 2, the damping parameter is not a constant at different bias fields. It is 0.018 at zero bias and then decreases with the increase of the longitudinal bias field, reaching a minimum value of 0.011 at a bias field of 2400 A/m (30 Oe). Then, the damping parameter increases steadily with the bias field beyond 2400 A/m (30 Oe).

Permeability spectra are obtained by performing an integration and then Fourier transformation of the time-domain data [6]. The two ferromagnetic resonance frequencies, the zero-crossing frequency and the peak frequency, show a steady increase with the longitudinal bias field, as indicated in Fig. 3. The zero-crossing ferromagnetic resonance frequencies f_0 at different bias fields $H_{\rm appl}$ can be fitted with the Kittel equation: $f_0 = (\gamma/2\pi)\mu_0\sqrt{M_s(H_k + H_{\rm appl})}$, where $\gamma = g\mu_B/\hbar$ is the gyromagnetic ratio, g is the Landé factor, μ_B is the Bohr magneton, $\hbar$ is Planck's constant, and M_s is the saturation magnetization [4]. A very interesting feature emerges, as shown in Fig. 3. At longitudinal bias fields larger than 1600 A/m (20 Oe), the zero-crossing frequencies can be fitted with a $B_s = 2.35$ T, an $H_k = 1280$ A/m (16 Oe), and a Landé factor of $g = 1.93$. The fitted H_k value is ~320 A/m (4 Oe) lower than the 1600 A/m (20 Oe) anisotropy field measured with a B–H loop tracer at a low frequency of 2 Hz. At zero bias, the peak ferromagnetic frequency is 2 GHz, which is very close to the value obtained from the Kittel equation, with a saturation magnetic induction of $B_s = 2.35$ T and an anisotropy field H_k of 1600 A/m (20 Oe).

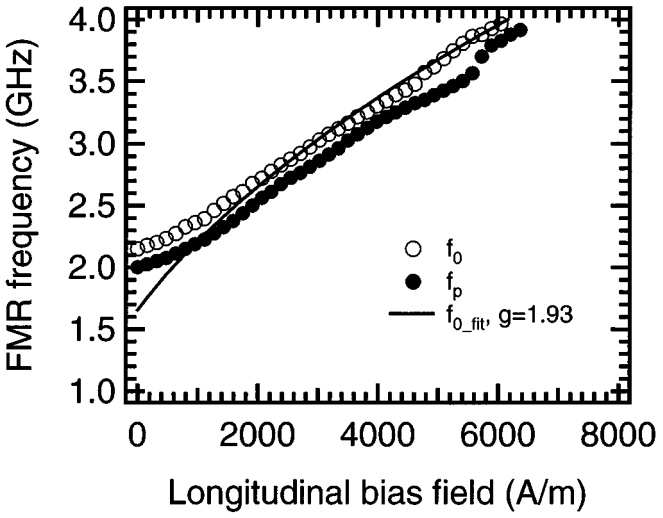

Fig. 3. The ferromagnetic resonance frequencies as a function of the longitudinal bias field. Open dots: the zero-crossing frequency. Solid dots: the peak frequency for the Fe–Co–N film. Solid line: the zero-cross frequency from fitting the Kittel equation for bias fields larger than 1600A/m (20 Oe), with $B_s = 2.35$ T, $H_k = 1280$ A/m (16 Oe). The obtained Landé factor g is shown in the graph.

The difference between the zero-crossing and peak frequencies *cannot* by explained by the simple model used here, which assumes that the film is a single, uniform magnetic domain. The explanation may stem from the presence of higher order magnetostatic modes [7].

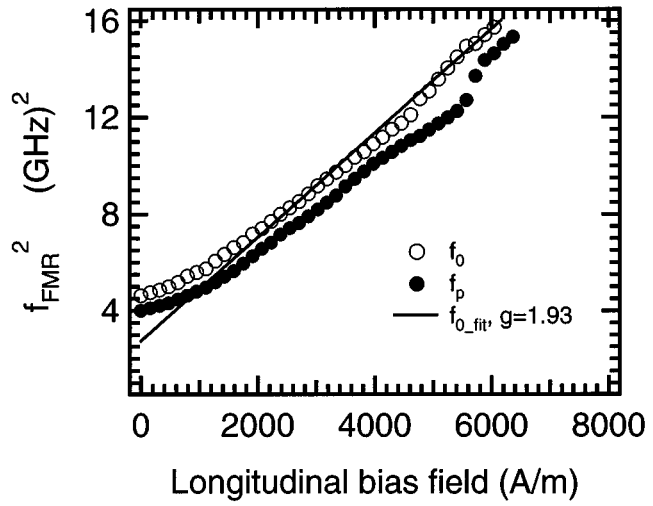

Fig. 4. The squared ferromagnetic resonance frequencies as a function of the longitudinal bias field. Open dots: the zero-cross frequency. Solid dots: the peak frequency for the Fe–Co–N film. Solid line is from a fit of (10) for bias fields larger than 1600 A/m (20 Oe), with $B_s = 2.35$ T, $H_k = 1280$ A/m (16 Oe). The obtained Landé factor g is shown in the graph.

The experimental data at low bias fields clearly deviate from the fitting curve, showing a *blue shift* with respect to the fitted ferromagnetic resonance frequencies. To better illustrate the blue shift at low bias, the squared ferromagnetic frequencies are plotted as a function of the bias field in Fig. 4. Clearly, the measured points depart from the fitted straight line. The ferromagnetic resonance frequency data at zero bias field, however, correspond well with an H_k value of about 1600 A/m f(20 Oe). This suggests that the effective anisotropy field decreases from about 1600 A/m (20 Oe) to about 1280 A/m (16 Oe) when an external DC bias field larger than 1600 A/m (20 Oe) is applied along the longitudinal direction.

III. Theoretical Analysis and Discussion

A. Small Signal Solution of the Landau–Lifshitz–Gilbert Equation

To better understand the data presented in the last section, we consider the Landau–Lifshitz–Gilbert (L–L–G) equation [8], [9] which is commonly used to describe magnetization dynamics

$$\frac{d\vec{M}}{dt} = -\gamma\vec{M} \times \vec{B} + \frac{\alpha}{M_s}\vec{M} \times \frac{d\vec{M}}{dt} \tag{1}$$

where the damping parameter α is a dimensionless phenomenological parameter: $\alpha = \lambda/\gamma\mu_0 M_s$.

If we assume a small-signal input (or a small excitation field), the L–L–G equation can be linearized and solved in the frequency domain (The details of the solution are in the Appendix.). For the case with longitudinal bias, an applied field $H_{\rm appl}$ is parallel to the easy axis, the susceptibility is

$$\chi(\omega) = \frac{\omega_m(\omega_m + \omega_k + \omega_{\rm appl} + j\omega\alpha)}{-\omega^2 + j\omega\alpha\omega_m + (\omega_k + \omega_{\rm appl})\omega_m} \tag{2}$$

where $\omega_{\rm appl} \equiv \gamma\mu_0 H_{\rm appl}, \omega_k \equiv \gamma\mu_0 H_k, \omega_m \equiv \gamma\mu_0 M_s$. In the case of a sinusoidal input $he^{j\omega_0 t}$ along the hard axis in time domain with the amplitude h, we get the magnetization along the hard axis as

$$m_x(\omega) = \chi(\omega) \times h \tag{3}$$

Making the substitution $s = j\omega$, where s is the complex independent variable for the Laplace transform and $j = \sqrt{-1}$, we obtain the transfer function (or the impulse response) of a magnetic thin film as follows:

$$\chi(s) = \frac{\omega_m(\omega_m + \omega_k + \omega_{\rm appl} + s\alpha)}{s^2 + s\alpha\omega_m + (\omega_k + \omega_{\rm appl})\omega_m}. \tag{4}$$

B. Phenomenology of Critical Damping

The transfer function represented by (4) can be regarded as the transfer function of a low-pass filter with two poles and one zero. The latter is a left-half-plane real zero far away from the two pole positions. Therefore, the high frequency characteristics of the transfer function will be mainly determined by the two poles in (4), similar to that of a two-pole low-pass filter [10]. The two poles can be found by setting the denominator to zero, and the two solutions are

$$s_{1,2} = \frac{1}{2}\left[-\alpha\omega_m \pm \sqrt{\alpha^2\omega_m^2 - 4\omega_m(\omega_k + \omega_{\rm appl})}\right]. \tag{5}$$

From the pole positions we can readily arrive at the damping condition for a magnetic film. If the two poles are complex numbers with nonzero imaginary parts, the transfer function is *underdamped*. If there are two real poles, the transfer function is *overdamped*. If there is only one real pole (degenerate poles), the transfer function is *critically damped* [10]. This occurs when the damping parameter is

$$\alpha_{\rm cri} = 2\sqrt{\frac{\omega_k + \omega_{\rm appl}}{\omega_m}} = 2\sqrt{\frac{1}{\chi_0}}. \tag{6}$$

where $\chi_0 = \chi(\omega = 0) = M_s/(H_k + H_{\rm appl})$ is the relative DC susceptibility. The value of the critical damping parameter depends not only on intrinsic material parameters but also on applied bias field. It increases with the increase of DC bias field along easy axis direction. For the Py/FeCoN film at zero bias field, $\chi_0 = 1000, \alpha_{\rm cri} = 0.06$. The measured damping parameters are all smaller than the critical value, so the film appears underdamped in the time domain data shown in Fig. 1.

In short, a *phenomenologial critical damping criteria* for a soft magnetic thin film under a *small signal* excitation field with a known DC susceptibility of χ_0 can be established as follows:

$$\begin{aligned} &\alpha > 2\chi_0^{-\frac{1}{2}}, \quad \text{overdamped} \\ &\alpha = 2\chi_0^{-\frac{1}{2}}, \quad \text{critically damped} \\ &0 < \alpha < 2\chi_0^{-\frac{1}{2}}, \quad \text{underdamped.} \end{aligned} \tag{7}$$

The utility of this criterion is that it provides a simple rule of thumb to determine when a soft magnetic film will be critically damped if we can independently adjust either the damping parameter or susceptibility. A determination of the necessary damping requires only a low-frequency measurement of the DC susceptibility, though an evaluation of the actual damping still

requires a high frequency measurement. Thus, such a criterion is convenient, but it does not explain the physics of damping, nor can it predict the damping for a given material.

The above critical-damping criterion for a soft ferromagnetic film under a small excitation field is contrasted with that of an isotropic ferromagnetic sphere, in which case the minimum remagnetization (the fastest large-angle switching) occurs at $\alpha = 1$ [11]. For an (in-plane) isotropic Permalloy thin film, the minimum remagnetization occurs at $\alpha = 0.013$ [11]. In the present case, for a Permalloy film with $M_s = 800$ kA/m and $H_k = 320$ A/m, a damping parameter of $\alpha = 0.04$ is required for it to be considered critically damped in the absence of DC bias field.

So far we have used *frequency domain* analysis to discuss critical damping. Alternatively, we can obtain equivalent results by analyzing the *time domain* solution of the small-signal transfer function of magnetic thin film. By getting the inverse Laplace transform of (4), we have the following time domain impulse response:

$$M(t) = M_0 \cdot \Theta(t) \cdot \left\{ \frac{\omega_m(\omega_m + \omega_k + \omega_{\rm appl}) + \alpha\omega_m s_1}{\sqrt{\alpha^2\omega_m^2 - 4\omega_m(\omega_k + \omega_{\rm appl})}} e^{s_1 t} + \frac{-\omega_m(\omega_m + \omega_k + \omega_{\rm appl}) - \alpha\omega_m s_2}{\sqrt{\alpha^2\omega_m^2 - 4\omega_m(\omega_k + \omega_{\rm appl})}} e^{s_2 t} \right\} \quad (8)$$

where $\Theta(t)$ is the Heaviside step function, and M_0 is a constant. The impulse response in time domain will be exponentially decreasing with time, i.e., *overdamped*, when the two pole s_1 and s_2 are real. If $s_1 = s_2$, we shall get a *critically damped* time domain impulse response: the impulse response will reach the equilibrium position in the shortest time, which is generally good for the system performance. When s_1 and s_2 are an imaginary conjugate pair, the impulse response will be a sinusoidal ringing curve with an exponentially decreasing envelope, i.e., *underdamped*.

C. Limitations of the Kittel Equation

The angular frequency for the underdamped sinusoidal impulse response is the nominal (angular) ferromagnetic resonance frequency, corresponding to the *peak frequency* of the imaginary part of (4). It is the same as the absolute value of the imaginary part of the two poles, i.e.,

$$\omega_p = \sqrt{\omega_m \left(\omega_k + \omega_{\rm appl} - \left(\frac{\alpha}{2}\right)^2 \omega_m \right)}. \quad (9)$$

In contrast, the *zero-crossing frequency* of the real part of (4) is

$$\omega_0 = \sqrt{\omega_m(\omega_k + \omega_{\rm appl})}. \quad (10)$$

This is the same as the Kittel equation used for fitting Figs. 3 and 4, also giving the nominal ferromagnetic resonance frequency [13]. In the absence of damping, (9) and (10) are identical. The zero-crossing frequency is approximately independent of the damping parameter α for a magnetic thin film, and larger than the peak frequency. This is *qualitatively* consistent with the data shown in Figs. 3 and 4. However, we find that the peak frequency data cannot be fitted with (9) with the same g-factor used for fitting the zero-crossing frequency, suggesting that damping alone is too small to account for the difference observed between the peak frequency and the zero-crossing frequency.

The Kittel equation has been widely used to obtain the anisotropy field H_k by extrapolating the squared ferromagnetic frequency as a function of the bias field [4], [13]. In this work, we extrapolate the squared zero-crossing frequency ω_0 to zero bias field to get the anisotropy field H_k for soft magnetic thin films. If we take the damping in magnetic thin films into account, the nominal ferromagnetic resonance frequency will be described by (9). Consequently, the Kittel equation will yield a measured anisotropy field which is slightly smaller than the real anisotropy field as follows:

$$H_k^{\rm measured} = H_k - \left(\frac{\alpha}{2}\right)^2 M_s. \quad (11)$$

For a damping parameter of $\alpha = 0.015$, however, the second term is about 100 A/m (1.3 Oe) for the Py/Fe–Co–N thin films. This is not large enough to explain why the effective anisotropy field at a bias field of >1600 A/m (20 Oe) is 1280 A/m (16 Oe), about 320 A/m (4 Oe) smaller than the value measured with a B–H loop tracer.

The experimental data and theoretical analysis indicate that the Py/FeCoN films studied here obey the Kittel equation *only qualitatively rather than quantitatively*. We believe that the single uniform magnetic domain model used to derive the Kittel equation and the small-signal solution of the L–L–G equation are oversimplified.

APPENDIX

The L–L–G equation is (in SI units)

$$\frac{d\vec{M}}{dt} = -\gamma\vec{M} \times \vec{B} + \frac{\alpha}{M_s}\vec{M} \times \frac{d\vec{M}}{dt}$$

If we assume that the easy axis and the bias field $H_{\rm appl}$ direction are along the y direction, and a small excitation field $he^{j\omega_t}$ is along the x direction, the magnetic film is in the x–y plane with the plane normal along the z direction, and the in-plane anisotropy field is small with respect to the saturation magnetization, i.e., $h \ll |H_k + H_{\rm appl}| \ll M_s$, then the magnetization can be expressed as

$$\vec{M} = M_s\hat{y} + (m_x\hat{x} + m_z\hat{z})e^{j\omega t}$$

where $|\vec{m}| \ll M_s$. The internal field is

$$\vec{H}_{\rm int} = he^{j\omega t}\hat{x} + (H_k + H_{\rm appl})\hat{y} - m_z e^{j\omega t}\hat{z}.$$

Substituting $\vec{M}$ and $\vec{H}_{\rm int}$ in the L–L–G equation with the above equations, removing the exponential term $e^{j\omega t}$, and neglecting the second-order small terms, we get the following relations along the x and z direction:

$$j\omega m_x = (j\omega\alpha + \omega_{\rm appl} + \omega_k + \omega_m)m_z,$$
$$j\omega m_z = \omega_m h - (\omega_{\rm appl} + \omega_k + j\omega\alpha)m_x.$$

Combining the above two equations, we obtain the relative permeability at an angular frequency of ω along the hard axis as

$$\chi \equiv \frac{m_x}{h} \approx \frac{\omega_m(\omega_{\mathrm{appl}} + \omega_k + \omega_m + j\omega\alpha)}{-\omega^2 + \omega_m(\omega_{\mathrm{appl}} + \omega_k + j\omega\alpha)}.$$

REFERENCES

[1] S. X. Wang, N. X. Sun, M. Yamaguchi, and S. Yabukami, "Sandwich films: Properties of a new soft magnetic material," *Nature*, vol. 407, p. 150, 2000.

[2] N. X. Sun and S. X. Wang, "Soft high saturation magnetization $(Fe_{0.7}Co_{0.3})_{1-x}N_x$ thin films for inductive write heads," *IEEE Trans. Magn.*, vol. 36, pp. 2506–2508, Sept. 2000.

[3] M. R. Freeman, M. J. Brady, and J. Smyth, "Extremely high frequency pulse magnetic resonance by picosecond magneto-optic sampling," *Appl. Phys. Lett.*, vol. 60, pp. 2555–2557, 1992.

[4] T. J. Silva, C. S. Lee, T. M. Crawford, and C. T. Rogers, "Inductive measurements of ultrafast magnetization dynamics in thin film permalloy," *J. Appl. Phys.*, vol. 85, pp. 7849–7862, 1999.

[5] K. B. Klaassen and J. C. van Peppen, "Exploring data rate limitations of channel front-ends for rigid disk drives," *IEEE Trans. Magn.*, vol. 37, pp. 619–626, Mar. 2001.

[6] C. Alexander, J. Rantschler, T. J. Silva, and P. Kabos, "Frequency- and time-resolved measurements of the FeTaN films with longitudinal bias fields," *J. Appl. Phys.*, vol. 87, pp. 6633–6635, 2000.

[7] N. X. Sun, S. X. Wang, and T. J. Silva, private communication.

[8] L. Landau and E. Lifshitz, "On the theory of the dispersion of magnetic permeability in ferromagnetic bodies," *Physik Z. Sowjetunion*, vol. 8, p. 153, 1935.

[9] T. L. Gilbert, "A Lagrangian formulation of the gyromagnetic equation of the magnetization field," *Phys. Rev. B*, vol. 100, p. 1243, 1955.

[10] A. V. Oppenheim and A. S. Willsky, *Signal and System*. Englewood Cliffs, NJ: Prentice-Hall, 1996.

[11] R. Kikuchi, "On the minimum of magnetization reversal time," *J. Appl. Phys.*, vol. 27, pp. 1352–1357, 1956.

[12] W. Bailey, P. Kabos, F. Mancoff, and S. Russek, "Control of magnetization dynamics in $Ni_{81}Fe_{19}$ thin films through the use of rare-earth dopants," *IEEE Trans. Magn.*, vol. 37, pp. 1749–1754, July 2001.

[13] C. Kittel, *Introduction to Solid State Physics*, 7th ed. New York: Wiley, 1996, p. 505.